Modern Physics Letters B
Vol. 35, No. 34 (2021) 2150510 (17 pages)

DOI: 10.1142/S0217984921505102

Effect of rolling deformation on microstructure and properties of Cu–Ni–Mo alloy prepared by aluminothermic reaction

Yuehong Zheng*, He Zhao†, Sijia Zhu‡, Peiqing La§, Faqi Zhan¶, Min Zhu‖, Jie Sheng** and Haibin Liu††

State Key Laboratory of Advanced Processing and Recycling of Nonferrous Metals, Lanzhou University of Technology, Lanzhou 730050, China

*zhengyuehong1986@126.com
†zh50911@163.com
‡1458147863@qq.com
§pqla@lut.edu.cn
¶756606724@qq.com
‖zhumin@lut.edu.cn
**shengj@163.com
††liuhb2160@163.com

Received 10 May 2021
Revised 11 August 2021
Accepted 5 September 2021
Published 14 October 2021

The metallic element Mo has almost no solid solubility in copper and can be used as a nucleation particle to refine the grain size and increase the recrystallization temperature of the alloy during solidification. It is expected to obtain copper alloys with good comprehensive properties by reasonably controlling the addition amount of Mo. However, it is difficult to prepare Cu–Mo alloys with uniform structure and there are few related literatures. In this paper, the aluminothermic reaction method, which has the advantages of simple process, low cost, and large size of the prepared alloy, was adopted, and a cluster model with the atomic ratio of Mo and Ni of 1:12 was introduced to design the alloy composition. Here, five alloys with different copper contents were prepared and followed by room temperature rolling with 40%, 60%, and 80% deformation. The results show that the as-cast Cu–Ni–Mo alloys exhibit good formability, have no macroscopic defects and present a small amount of precipitates. With the increase of alloy elements Ni and Mo, the hardness and strength of the alloys increase obviously, while the electrical conductivity decreases gradually. For the rolled alloys, a large number of lamellar deformed structures are formed, the grains are obviously refined, the precipitated phases are broken and the distribution is more uniform, thus the strength and hardness of the alloy increase significantly, the plasticity decrease significantly, while the conductivity changed little. In this study, high-strength samples were obtained, which may be a valuable exploration for the preparation of Cu–Ni–Mo alloy sheets with excellent microstructure and mechanical properties.

Keywords: Aluminothermic reaction; copper alloy; rolling; mechanical property; conductivity.

*Corresponding author.

1. Introduction

Cu and its alloys with excellent electric and thermal conductivity, corrosion resistance and good process ability, have been widely used in power transmission, electronic communications, machinery manufacturing, decorative craft and many other areas.[1,2] However, their tensile strength and yield strength at room temperature and high temperature are low, which cannot meet the needs of some special industries. For example, when the copper alloy is used as the lead frame of the integrated circuit and the overhead contact wire of high-speed railway,[3] it is required to have the characteristics of high strength and high conductivity at the same time. However, these two properties are a pair of contradictions.[4] Therefore, how to balance these properties has always been one of the research directions in the field of copper alloys.

Among many methods to balance these properties, controlling the solid solution and precipitation of elements in the alloy is the most common.[4,5] Solid solution strengthening mainly produces stress field by lattice distortion due to the difference of atomic size between solute and matrix, and interacts with the elastic stress field around dislocations to hinder the movement of dislocations, so as to improve the strength. However, the more serious the lattice distortion is, the stronger the scattering effect on electrons is, and the more the loss of conductivity is.[6] For instance, the tensile strength of as-cast Cu-3wt.%Al and Cu-7wt.%Al alloys increases with the increase of alloying element content, which are 240 MPa and 310 MPa, respectively, while the conductivity is opposite, which are 21 %IACS and 16 %IACS,[7] respectively. However, the tensile strength of Cu-0.2wt.%Mg and Cu-0.4wt.%Mg alloys is 269 MPa and 277 MPa, respectively. The electrical conductivity of Cu-0.2wt.%Mg and Cu-0.4wt.%Mg alloys decreases with the increase of alloying elements, but still remains at a high level, 95 %IACS and 83 %IACS,[8] respectively. It can be seen that the type and concentration of solute atoms are crucial to balance the strength and conductivity of copper alloys. Precipitation strengthening is to use a large number of second relative dislocations in the matrix to play the role of pinning effect, reduce the concentration of solute and the degree of lattice distortion, and improve the electrical conductivity while increasing the strength.[9] For example, after aging at 475°C for 30 min, Cu-0.80%Cr-0.080%Zr (wt.%) alloy is evenly distributed with small size Cr and Zr precipitates in the matrix, with a hardness of 162 $HV_{0.5}$ and conductivity of 75 %IACS.[10] However, for elements such as W and Mo, which are almost insoluble in Cu, the studies show that it is difficult to disperse in the Cu matrix for those elements, and tend to show the phenomenon of segregation, which cannot improve the properties of the alloy.[6,11] Even the special preparation method cannot improve the segregation phenomenon, for example, the Cu-20%Mo alloy prepared by mechanical ball milling method contains a large number of pores in the matrix, and Mo element is enriched, the conductivity is only between 20.3 %IACS and 24.8 %IACS.[6] The Cu–Mo films with different Mo content prepared by DC magnetron sputtering are not uniform, and there are Mo rich regions.[12]

Our research group also tried to prepare Cu–Mo binary alloy by aluminothermic reaction method in the early stage, however, there are many holes in the alloy macroscopically, and Mo segregation was serious. Namely, it is difficult to obtain alloy with uniform composition when Mo and other insoluble elements are directly added to Cu.

In order to effectively control the solid solution and precipitation of Mo and other insoluble elements in Cu matrix, Chuang Dong's research group[13,14] proposed a model of "cluster plus glue atoms" for alloy composition design. Studies have shown that in the Cu–Ni–M alloy system (M stands for different metallic elements), if M is a transition metal element with positive mixing enthalpy with Cu and negative mixing enthalpy with Ni, and when the atomic ratio of M to Ni is 1:12, it can constitute an ideal situation of short-range ordered local structure. That is, the alloying elements can form $[M_1Ni_{12}]$ cubic octahedral clusters with M atoms as the center and Ni atoms as the first neighbor, and scattered in the Cu substrate to form stable solid solution alloys. On this basis, further adjusting the atomic ratio of M to Ni can effectively control the solid solution and precipitation of M element.[15,16] When Mo was used as the third component M,[17,18] Cu–Ni–Mo alloy system with controllable solid solution and precipitation of Mo element could be formed by vacuum arc melting and magnetron sputtering, meanwhile, the influence of Mo and Ni in cluster solution on the electrical conductivity of the alloy was also studied. However, the size of the alloy prepared by these two methods is limited. Therefore, this paper aims to further explore the method of preparing Cu–Ni–Mo alloy with large size and the influence of subsequent deformation on the structure and properties-based on the design composition of cluster model.

In our previous research, a series of large-size steel[19,20] and Fe–Al–Cr alloys[21] with micro-nanostructure have been prepared by aluminothermic reaction method, which is energy saving and environmental protection, simple process and low cost. Therefore, this preparation process can be further extended to the preparation of copper alloys, but in order to further improve the strength of the alloy prepared by the thermite method, increase the size of the material and eliminate casting defects, the alloy usually needs to be further rolled. The increasing dislocation density in the crystal during plastic deformation will increase the probability of dislocation pile-up group, jogs and entanglement, hinder the further movement of dislocations, so as to improve the strength of the alloy. However, due to insufficient movement of dislocations, the plasticity of the alloy will decrease significantly. Meanwhile, the rapid increase of dislocation density and lattice distortion caused by rolling will have a negative impact on the electrical conductivity of the alloy.[7,8] The study shows that after rolling of 96% deformation at room temperature, the tensile strength of pure copper increases from 206.2 MPa in the initial state to 419.0 MPa, but the elongation decreases from 50.8% to 6.8%, and the electrical conductivity decreases from 96.86 %IACS to 84.10 %IACS.[22] When the Cu-10wt.%Fe alloy is rolled with 98% deformation at room temperature, the tensile strength increases from 340 MPa to 543 MPa, the elongation decreases from 19.0% to 3.1%, and the electrical

conductivity decreases from 31.2 %IACS to 13.5 %IACS.[23] The hardness of Cu–3Ti–2Mg (wt.%) alloy increases from 160 HV to 279 HV and the electrical conductivity decreases from 5.0 %IACS to 4.2 %IACS after the alloy is rolled at room temperature with a deformation of 70%.[24] It can be seen that the exploration of subsequent deformation process is particularly important to obtain the evolution law of copper alloy properties. Undoubtedly, the change of properties of the rolled alloy is necessarily accompanied by the evolution of microstructure or texture, therefore, the microstructural evolution of rolled copper[25,26] and alloys of similar structure (Al[27] and Ni[28,29]-based alloys) is also the focus of researchers.

Therefore, this paper is based on the solid solution cluster model, the ratio of Mo and Ni in the alloy is designed to be 1:12, which aims to uniformly distribute the insoluble Mo element in the Cu matrix through the strong interaction of Ni. Then the Cu–Ni–Mo ternary alloys with a large size are prepared by the aluminothermic reaction method with CuO and Al as main raw materials. Finally, the effect of rolling deformation on the microstructure and properties of the alloy is discussed in detail.

2. Experimental Procedure

In this paper, Cu–Ni–Mo ternary alloys were prepared by aluminothermic reaction method. Generally, aluminothermic reaction equation of Cu preparation is shown in Eq. (1), but the reaction system has a high adiabatic combustion temperature (T_{ad}) of 5151 K. In order to reduce T_{ad}, part of Cu powder is used as a diluent, and the reaction equation is shown in Eq. (2).

$$3CuO + 2Al = Al_2O_3 + 3Cu, \tag{1}$$

$$2Al + 3CuO + 4Cu = Al_2O_3 + 7Cu. \tag{2}$$

In order to meet the requirements of component design of the clusters model, the atomic ratio of Mo to Ni is fixed at 1:12, then change the total amount of the alloying elements at the same time, the design component of Cu–Ni–Mo ternary alloy series can be obtained. Then according to the Eq. (2) and design composition of the alloy, the weight of the reaction materials (CuO, Al, Ni, Mo and Cu powders) required for the preparation of 1 kg alloy can be calculated, as shown in Table 1. The purity of all the raw materials is more than 99 wt.%, and the average particle size is 74 μm.

The concrete steps of alloy preparation are as follows: First, the raw material of the reactant was weighed according to the proportion by the electronic balance, and loaded into the sealed tank of QM-1SP4 planetary ball mill with the ratio of ball to material of 1:2 for ball grinding for 8 h, the rotation speed is 180 r/min, and the ball grinding beads are Al_2O_3 balls. Then the reaction raw material after ball milling was placed in a cylindrical stainless steel mold, which was pressed into a number of cylindrical billets under the pressure of 70 MPa for 5 min on uniaxial press, and then placed in a graphite crucible. Then, 4 g of kindling agent was pressed

Table 1. Composition of Cu–Ni–Mo alloys designed-based on cluster model and weight of reactant powders.

Alloys	Composition (at.%)			Total content of alloying elements (at.%)	Raw materials (g)				
	Cu	Ni	Mo		CuO	Al	Mo	Ni	Cu
$Cu_{99}[Ni_{12/13}Mo_{1/13}]_1$	99.00	0.92	0.08	1.00	531.28	120.13	1.20	8.50	565.89
$Cu_{97}[Ni_{12/13}Mo_{1/13}]_3$	97.00	2.77	0.23	3.00	520.84	117.77	3.50	25.60	554.81
$Cu_{95}[Ni_{12/13}Mo_{1/13}]_5$	95.00	4.62	0.38	5.00	510.45	115.42	5.70	42.70	543.70
$Cu_{93}[Ni_{12/13}Mo_{1/13}]_7$	93.00	6.46	0.54	7.00	500.01	113.06	8.20	59.80	532.59
$Cu_{90}[Ni_{12/13}Mo_{1/13}]_{10}$	90.00	9.23	0.77	10.00	484.33	109.52	11.70	85.50	515.88

into a sheet and placed on the top of the raw material billet, and the door of the high-pressure reaction kettle was closed. Finally, under the protection of 5 MPa Ar, when the temperature in the high-pressure reactor reaches 260°C, the kindling agent is ignited to release a large amount of heat, thus triggering the thermite reaction. After the reaction, the sample is taken out after the furnace cools to room temperature.

The as-cast alloy was processed into three groups of samples with the size of $80 \times 20 \times 8$ mm^3 by electric spark wire cutting machine, and then rolled by two-high hot and cold rolling mill in multiple passes at room temperature with the reduction of 0.05 mm in each pass, which reduced the thickness of the three groups of samples by 40%, 60% and 80%, respectively.

The microstructure of the alloy was observed by Zeiss LSM800 laser scanning confocal microscope, and the microstructure and elemental surface scanning were analyzed by Quanta FEG450 scanning electron microscope (SEM) and its accessory X-ray energy dispersion spectrum (EDS). The structure of the alloy was characterized by D8 Advance X-ray Diffraction (XRD), the scanning voltage is 40 kV and current is 40 mA. The conductivity of the alloy was measured by digital eddy current metal conductance instrument Sigma2008B/C at room temperature, and 10 points were measured for each sample to take the average value. Wilson-VH1102 automatic microhardness testing system was used to test the Vickers hardness of

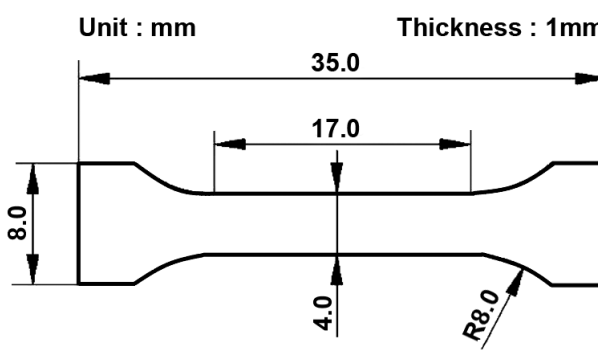

Fig. 1. Dimensional diagram of tensile specimen.

the alloy. The load was 10 mN and the loading time was 10 s. The average value of 10 points of each group of samples was taken as the final result. At room temperature, the displacement loading method was used to carry out the tensile test on Shimazu AGS-X 300 kN electronic universal testing machine, and the rate is 0.1 mm/min. Three parallel experiments were conducted for each group of samples. The size of the tensile sample is reduced in the same proportion according to the national standard GB/T 228.1-2010 (Tensile Tests for Metallic Materials Part 1: Experimental Methods at Room Temperature), and the size diagram is shown in Fig. 1.

3. Results

Figure 2 shows the metallographic structure of as-cast and rolled Cu–Ni–Mo alloys. The alloys are continuous and compact in macroscopic condition, without obvious pores or large area enrichment of alloying elements, which preliminarily indicate that the Cu–Ni–Mo alloys prepared by the thermite method-based on cluster model design can effectively avoid the disadvantage of poor formability of Cu–Mo binary alloys. Through comparative analysis, the grain size of as-cast alloys (Figs. 2(a)–2(e)) decreases with the increase of alloying element content. The main reasons are as follows: First, with the increase of alloying element content, the adiabatic temperature of the reaction system decreases, the solidification and cooling time of the alloy become shorter, and the growth time after grain nucleation becomes shorter; second, with the increase of Ni content, more Mo atoms will be dissolved into the Cu matrix, and the solid solution Mo in the matrix can be used as the crystallization core to refine the grain. In addition, a small amount of fine precipitates are uniformly distributed in the as-cast alloy. The grains and precipitates are elongated along the rolling direction with the rolling deformation increased (Figs. 2(a-1)–2(a-3), 2(b-1)–2(b-3) and 2(c-1)–2(c-3)), and a large number of fibrous deformation bands are eventually formed.

Figure 3(a) shows the XRD pattern of as-cast Cu–Ni–Mo alloys. The diffraction patterns are composed of the diffraction peaks of Cu and Mo, indicating that Mo atoms in the as-cast alloys are not completely dissolved in the matrix, and some Mo exists in the form of precipitated phase. Figure 3(b) shows the XRD patterns of $Cu_{97}[Ni_{12/13}Mo_{1/13}]_3$ alloy after rolling with different deformations. With the increase of deformation, the composition of the diffraction pattern has almost no change, indicating that the rolling process has little effect on the phase transformation, but the FWHM of each diffraction peak increases gradually after rolling, indicating that the stress concentration occurs in the grain, which leads to dislocation pile-up and significant increase of alloy defects.

Figure 4 shows the SEM image and the corresponding EDS surface scanning element distribution of as-cast and rolled $Cu_{97}[Ni_{12/13}Mo_{1/13}]_3$ alloys. As can be seen from Fig. 4(a), the grain size of the as-cast alloy is large and there are small granular precipitates in the grain. However, the EDS surface scanning results show

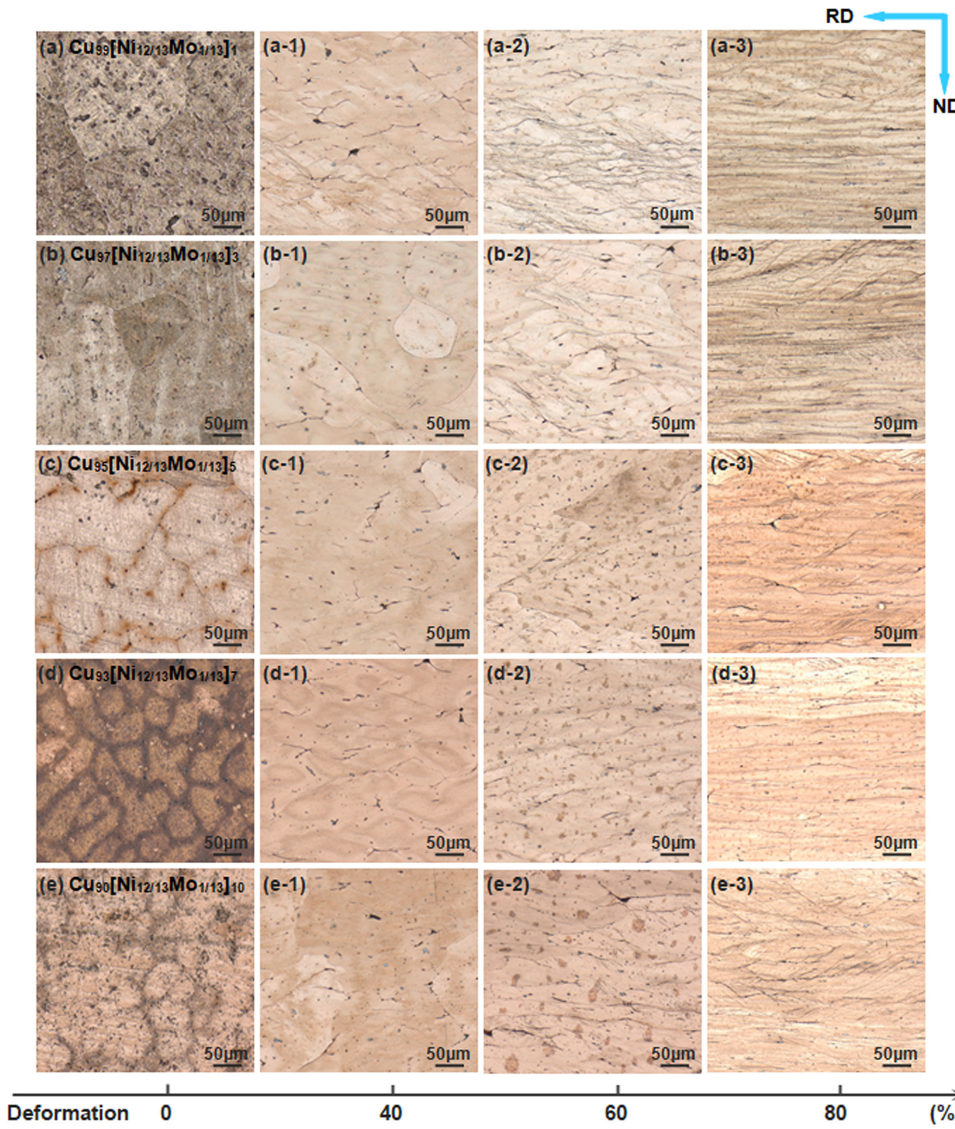

Fig. 2. (Color online) Metallographic structure of as-cast and rolled Cu–Ni–Mo alloys: $Cu_{99}[Ni_{12/13}Mo_{1/13}]_1$(a)–(a-3), $Cu_{97}[Ni_{12/13}Mo_{1/13}]_3$(b)–(b-3), $Cu_{95}[Ni_{12/13}Mo_{1/13}]_5$(c)–(c-3), $Cu_{93}[Ni_{12/13}Mo_{1/13}]_7$(d)–(d-3) and $Cu_{90}[Ni_{12/13}Mo_{1/13}]_{10}$ (e)–(e-3). (The sample with 0% deformation denotes the as-cast sample.)

that the introduction of Ni element can make most of Mo dissolved into the Cu matrix, and only a very small amount of Mo is precipitated out. As the amount of rolling deformation increases (Figs. 4(b)–4(d)), the grains are elongated and broken along the rolling direction, and the grain size decreases, forming a large number of deformation textures, and the grain boundary changes from clear to fuzzy. After

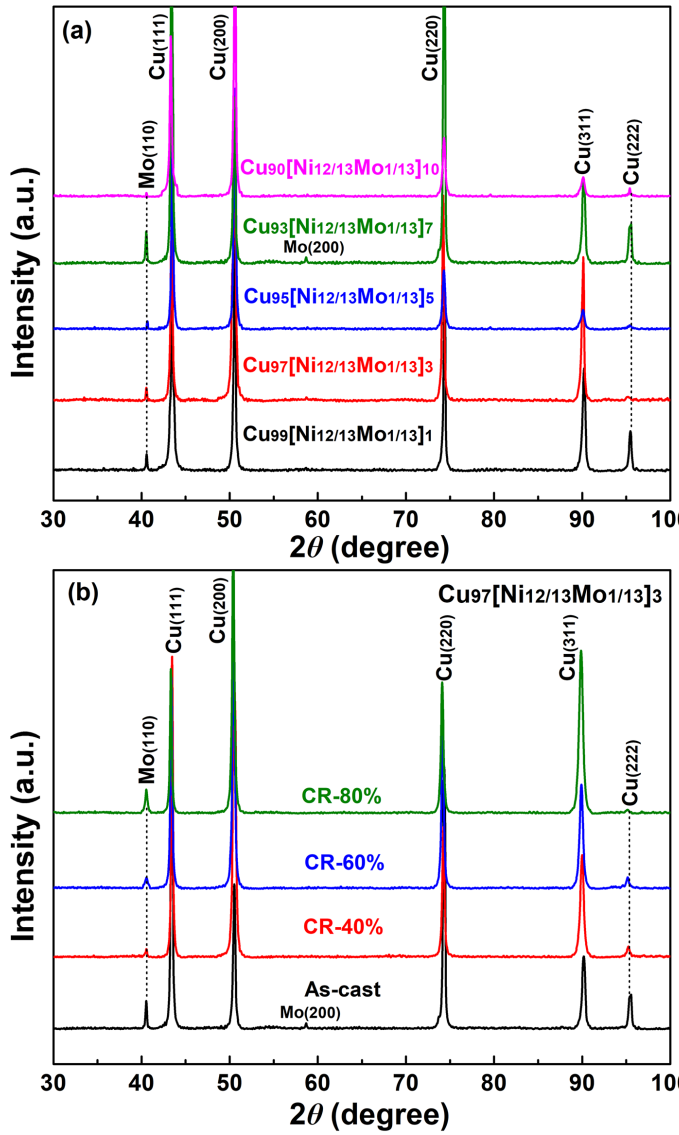

Fig. 3. (Color online) XRD patterns of as-cast Cu–Ni–Mo alloys (a) and the $Cu_{97}[Ni_{12/13}$-$Mo_{1/13}]_3$ alloy after rolling with different deformations (b).

rolling with 80% deformation (Fig. 4(d)), the size of precipitated Mo particles is significantly reduced and the distribution in Cu matrix is more uniform.

Figure 5 shows the variation curves of hardness of Cu–Ni–Mo alloys with rolling deformation. It can be seen that the hardness of the alloy increases with the increase of alloy element content under the same deformation condition. The hardness with the same composition increases significantly with the

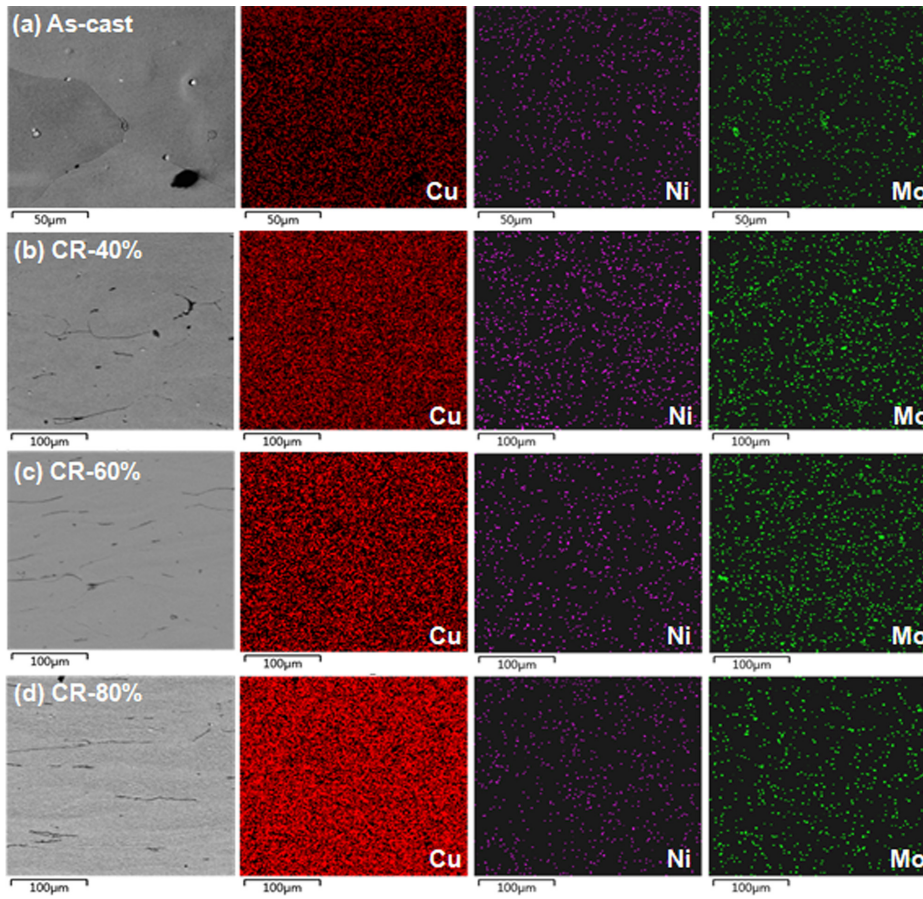

Fig. 4. (Color online) EDS surface scanning element distribution results of as-cast and rolled $Cu_{97}[Ni_{12/13}Mo_{1/13}]_3$ alloys: (a) as-cast, (b) 40% rolling, (c) 60% rolling and (d) 80% rolling.

increase of deformation degree. The hardness of $Cu_{99}[Ni_{12/13}Mo_{1/13}]_1$, $Cu_{97}[Ni_{12/13}Mo_{1/13}]_3$ and $Cu_{95}[Ni_{12/13}Mo_{1/13}]_1$ alloys with relatively low alloy element content increases slowly after rolling with 60% and 80% deformation. The hardness of $Cu_{93}[Ni_{12/13}Mo_{1/13}]_7$ and $Cu_{90}[Ni_{12/13}Mo_{1/13}]_{10}$ alloys with higher alloying degree increases linearly with the increase of deformation.

Figure 6 shows the variation curves of the conductivity of Cu–Ni–Mo alloys with the amount of rolling deformation. It can be seen that the conductivity of the alloy decreases with the increase of alloy element content with the same amount of deformation. The conductivity of $Cu_{99}[Ni_{12/13}Mo_{1/13}]_1$ and $Cu_{97}[Ni_{12/13}Mo_{1/13}]_3$ alloys decrease slightly compared with that in cast state. However, the conductivity increases slightly or even does not change when the rolling deformation increases to 60% and 80%. But the conductivity of $Cu_{95}[Ni_{12/13}Mo_{1/13}]_5$, $Cu_{93}[Ni_{12/13}Mo_{1/13}]_7$ and $Cu_{90}[Ni_{12/13}Mo_{1/13}]_{10}$ alloys remains basically unchanged after rolling.

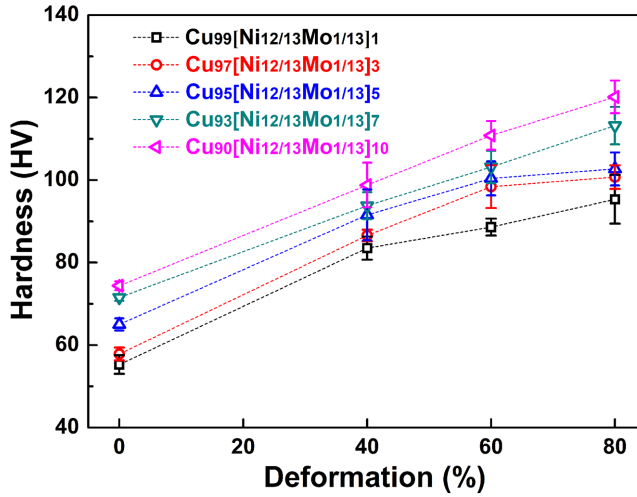

Fig. 5. (Color online) Variation curves of hardness of Cu–Ni–Mo alloys with rolling deformation.

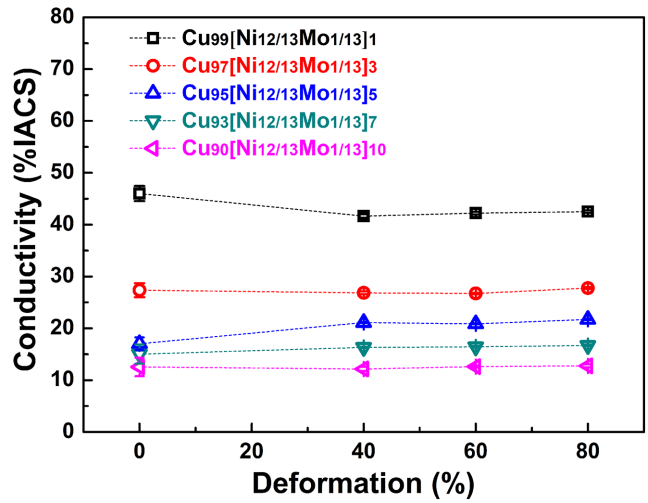

Fig. 6. (Color online) Variation curves of conductivity of Cu–Ni–Mo alloys with rolling deformation.

Figure 7 shows the stress–strain curves of Cu–Ni–Mo alloy under different rolling deformation conditions and the corresponding variation curves of tensile strength and elongation. Compared with the as-cast sample, the tensile strength of each sample is significantly increased after rolling, and the strength increases with the increase of deformation. However, the elongation decreases sharply after rolling with 40% deformation, and the decrease range increases with the increase of alloy element content. But with the increase of rolling deformation, the decrease range becomes smaller. The variation trend of the tensile strength and elongation of Cu–Ni–Mo

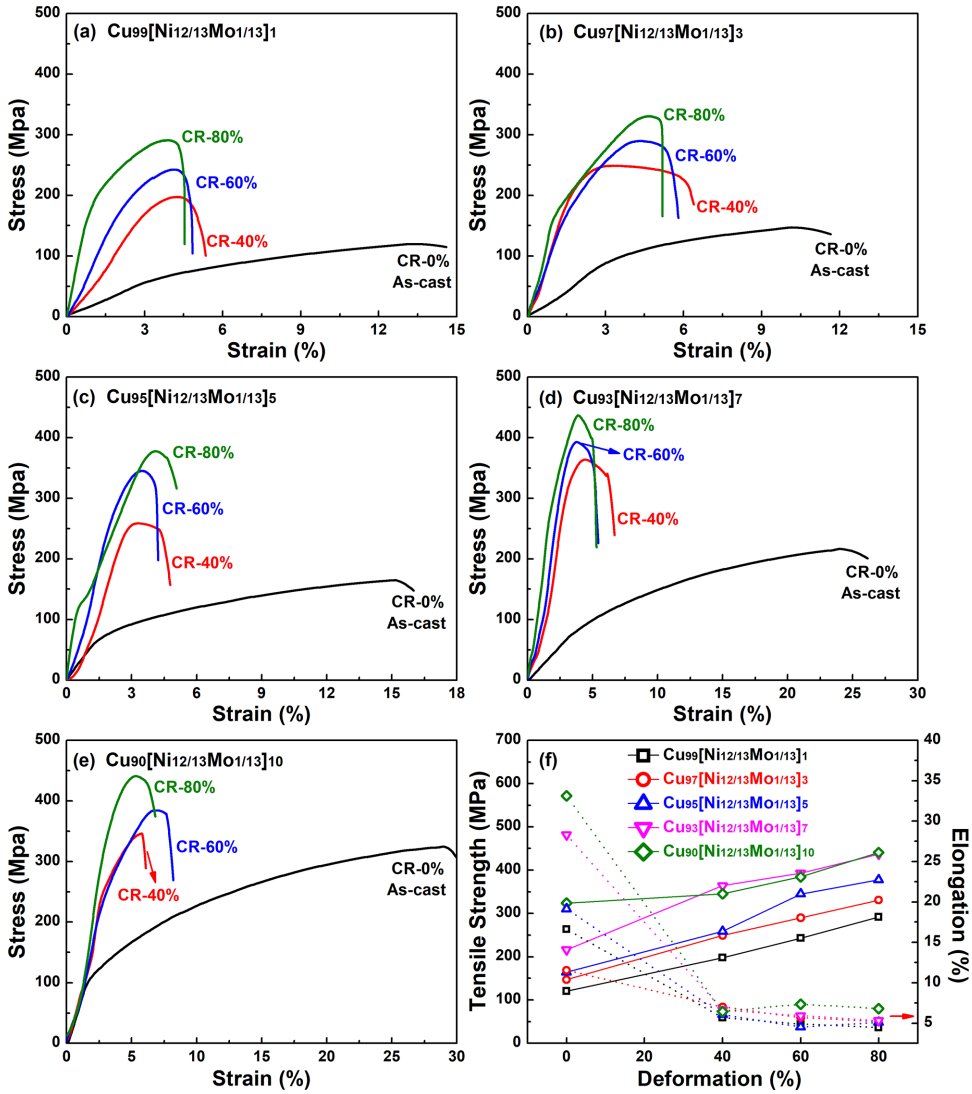

Fig. 7. (Color online) Stress-curves of $Cu_{99}[Ni_{12/13}Mo_{1/13}]_1$ (a), $Cu_{97}[Ni_{12/13}Mo_{1/13}]_3$ (b), $Cu_{95}[Ni_{12/13}Mo_{1/13}]_5$ (c), $Cu_{93}[Ni_{12/13}Mo_{1/13}]_7$ (d) and $Cu_{90}[Ni_{12/13}Mo_{1/13}]_{10}$ (e) alloys after rolling with different deformations and their corresponding tensile strength and elongation (f).

alloy with different components after rolling with different deformations at room temperature is shown in Fig. 7(f). The tensile strength of $Cu_{93}[Ni_{12/13}Mo_{1/13}]_7$ alloy after rolling with 80% deformation increases by 220.64 MPa and the elongation decreases by 23.02% compared with the as-cast alloy.

Figure 8 shows the tensile fracture morphology of $Cu_{90}[Ni_{12/13}Mo_{1/13}]_{10}$ alloy after rolling with different deformations. It can be seen that the tensile fracture

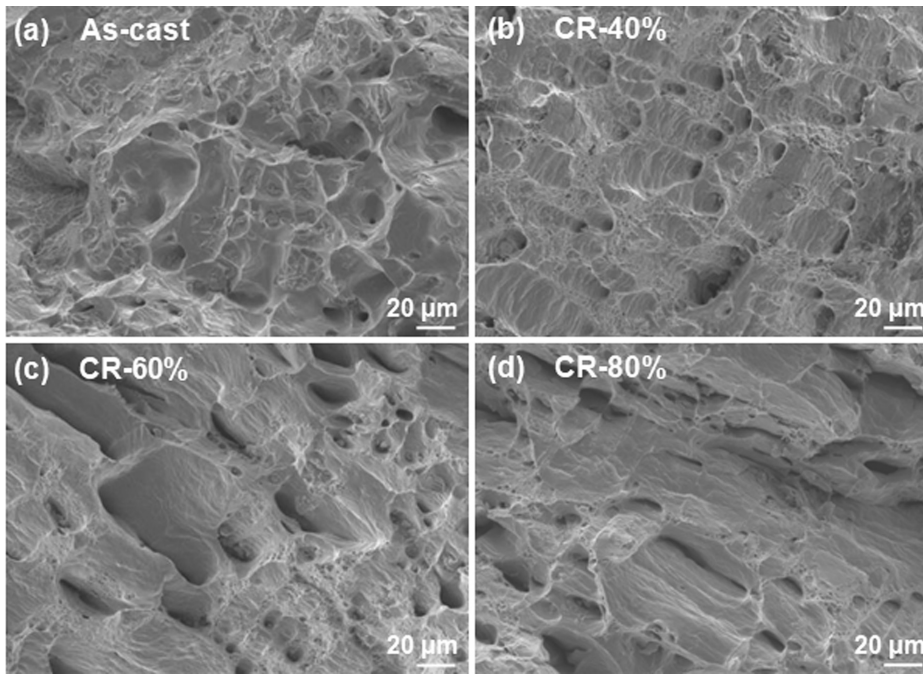

Fig. 8. Tensile fracture morphologies of $Cu_{90}[Ni_{12/13}Mo_{1/13}]_{10}$ alloys after rolling with different deformations: (a) as-cast, (b) 40% rolling, (c) 60% rolling and (d) 80% rolling.

dimples of the as-cast alloy is small with the largest number, and there are a small amount of precipitates in the dimples, indicating that the alloy has good toughness and is characterized by ductile fracture (Fig. 8(a)). After rolling with 40% deformation, the number of shallow dimples in the fracture is significantly reduced, and the size of dimples becomes larger, showing the characteristics of mixed ductile-brittle fracture, with tearing edge and river pattern (Fig. 8(b)). With the increase of rolling deformation, fracture dimples further decrease and are mainly composed of dissociation planes, showing quasi cleavage fracture mode (Fig. 8(d)).

4. Discussion

4.1. *Reaction mechanism and tissue structure analysis*

In general, the T_{ad} of the aluminothermic reaction system (Eq. (1)) for preparing Cu is 5151 K, but adding an appropriate amount of copper powder to the reaction powder can reduce the T_{ad} of the system and accelerate the reaction process. When the mole ratio of CuO to pure Cu is 3:4, the T_{ad} of the reaction system (Eq. (2)) decreases to 3273 K, but this temperature is still higher than the melting point of the refractory metal Mo (2893 K). In the process of aluminothermic reaction, the mixed melt of Al_2O_3 and Cu can be regarded as an unstable emulsion. At the moment of completion of the reaction, numerous small Al_2O_3 droplets are dispersed in the

Cu melt, and these droplets will collide with each other and aggregate into large droplets to reduce the interface energy. The higher the volume fraction of Al_2O_3, the more chances of collision. The droplet aggregation rate can be described by the von Smoluchowsky equation.[30]

$$\frac{dV_{\text{ave}}}{dt} = \frac{4k \cdot T \cdot V}{3\eta} \exp\left(-\frac{E_A}{k \cdot T}\right), \tag{3}$$

$$\eta(T) = \eta_0 \exp\left(\frac{A}{T - T_0}\right), \tag{4}$$

where V_{ave} represents the average volume of Al_2O_3 droplets, V is the volume fraction of Al_2O_3 droplets in the mixed melt, T is the absolute temperature, k is the Boltzmann constant, η is the viscosity of copper melt, E_A is the mechanical barrier, T_0 is the liquid–solid transition temperature, η_0 is the viscosity corresponding to the liquids of the alloy. From Eqs. (3) and (4), it can be seen that η and dV_{ave}/dt increase with the rise of temperature. Compared with Cu–Mo binary alloy, Ni is the main alloying element in Cu–Ni–Mo alloy with less Mo content, and melting heat of Ni (17.61 kJ/mol) is far lower than that of Mo (32.0 kJ/mol), namely, Ni absorbs less heat than Mo by melting, and has less influence on T_{ad} of the system, η and dV_{ave}/dt are relatively higher, so Cu melt and Al_2O_3 droplet can be effectively separated. According to the mixing enthalpy,[31] it can also be known that the mixing enthalpy of Mo and Ni is negative and that between Mo and Cu is positive. Therefore, there is a high probability that Mo and Ni atoms are adjacent, and it is easy to form $[Mo_1Ni_{12}]$ cubic octahedral clusters with Mo atom as the center and Ni atom as the first nearest neighbor, which is solidly soluble in the Cu matrix. In addition, due to the high thermal expansion coefficient of Al_2O_3, the density difference between Al_2O_3 and Cu alloy melt is large with liquid state, and it will automatically float to the top of copper melt after solidification. Therefore, bulk Cu–Ni–Mo ternary alloys with complete macroscopic morphology and large size can be prepared by the thermite method.

However, according to the composition and structure analysis, a small amount of Mo precipitates in the form of the second phase in the Cu–Ni–Mo alloy designed and prepared-based on the cluster model, and does not achieve complete solid solution. This is because the reaction temperature reaches 3273 K, and part of Ni evaporates, resulting in the ratio of Mo to Ni is greater than the solid solution cluster ratio of 1:12. According to the literature,[17,18] the excess Mo is not dissolved in the matrix in the form of clusters, but in the state of elemental precipitation. In addition, further subsequent heat treatment will also affect the diffusion of atoms and further promote the solid solution of Mo atoms, which needs to be further explored in the future.

4.2. *Mechanism of action of microstructure on strength*

The strengthening of as-cast Cu–Ni–Mo alloy is mainly due to the solid solution of $[Mo_1Ni_{12}]$ clusters formed by Ni and Mo atoms into the Cu matrix. Stress field is generated around the clusters, which interacts with the elastic stress field around the dislocation to block the dislocation motion and produce solid solution strengthening effect. The grains of the rolled Cu–Ni–Mo alloy are elongated along the rolling direction with the increase of the deformation amount, and the large grains are gradually broken up, the number of grain boundaries increases, and a large number of deformation textures are produced. The size of the Mo phase precipitated initially decreases obviously, and the distribution in the Cu matrix is more uniform, as shown in Fig. 9. In the process of cold deformation, the phenomenon and mechanism of polycrystalline grains of face centered cubic alloy being refined have been reported in literatures,[32,33] that is, although the grains in each region during the deformation process, fewer slip systems operate than specified by the Taylor criterion for strain accommodation, taken collectively, the slip in a group of adjacent volume elements acts approximately to fulfill this criterion. This slip pattern leads to a subdivision of grains. The subdivision occurs on a smaller and smaller scale with increasing deformation.[32] Obviously, the increased grain boundaries will hinder the dislocation movement and produce a strengthening effect to improve the deformation resistance. When the alloy is rolled, the cold plastic deformation force causes the dislocation source inside the grain to actuate, and a large number of dislocation plugs are formed at the grain boundary to generate the stress field, which activates the dislocation source inside the adjacent grain and improves the strength. At the same time, due to the dislocation cannot fully move, plasticity decreased significantly. With the continuous increase of rolling deformation, the dislocation continues to proliferate, which leads to more prominent dislocation packing group, jogs and entanglement, resulting in the increase of strength and the decrease of plasticity.

Apparently, the influence of precipitated particles on strength cannot be ignored. In the as-cast Cu–Ni–Mo alloy, there are Mo particles precipitated with higher hardness, they are difficult for dislocation to cut through. Under the action of external force, the dislocation line will bypass the precipitation particles, which

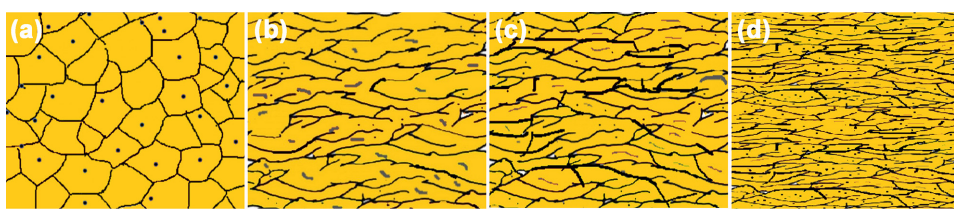

Fig. 9. (Color online) Evolution mechanism of internal grains and precipitates in Cu–Ni–Mo alloy during rolling process.

is the Orowan bypass mechanism.[34,35] However, this precipitation strengthening effect increases with its decreasing size and increasing volume fraction under the bypassing mechanism. Therefore in as-cast alloys, the precipitation strengthening effect is not outstanding due to the large size of precipitated particles. In the rolled alloys, the Mo particles are broken and dispersed, especially in the rolling direction, the distribution of Mo particles is more uniform, the particle spacing decreases, and the volume fraction increases, thus the strengthening effect of precipitation on the alloy matrix increases, and the strengthening effect becomes more obvious with the increase of the rolling deformation. According to the literature,[36] this similar strengthening phenomenon also exists in the rolled high entropy alloys, i.e. a nanolamellar microstructure with fragmented Laves phase particles arranged preferentially along the rolling direction and the intense deformation zones surrounding the hard Laves phase particles, which contributed to significant increases in both tensile strength and yield strength of cold rolled high entropy alloys.

4.3. *Mechanism of action of microstructure on electrical conductivity*

The main factor affecting the conductivity of as-cast Cu–Ni–Mo alloy is the lattice distortion caused by solute atoms in the matrix, which destroys the periodicity of the dot matrix potential field, and thus produces strong scattering effect on the directional motion of electrons, resulting in the decrease of the conductivity of the alloy. For alloys with low solute content, the relationship between the resistivity ρ of the alloy and solute atoms can be approximately described according to the theory of conductivity[37]:

$$\rho = \rho_0 + \rho_S = \rho_0 + C \cdot \Delta\rho, \tag{5}$$

where ρ_0 is the pure metal resistivity, C represents the concentration of solute atoms, $\Delta\rho$ is the additional resistivity produced by 1 at.% solute atoms. As the atomic cluster of alloy element $[Mo_1Ni_{12}]$ increases from 1 at.% to 10 at.%, the lattice distortion and the scattering effect on electrons are increased. Therefore, the conductivity of Cu–Ni–Mo alloy decreases with the increase of alloying element content.

The cold plastic deformation occurs in rolled Cu–Ni–Mo alloy results in the increase of dislocation density, the increase of lattice distortion degree and the increase of electron scattering probability. The grain size is refined, the number of grain boundaries increases, and the scattering effect of electrons by grain boundaries increases, which have an adverse effect on the conductivity of the alloy. The point defect concentration of the alloy decreases gradually and the scattering effect of the point defect on the electron is reduced by rolling. With the rolling progress, the size of the precipitated phase decreases obviously, the volume fraction increases and the distribution shows more uniform, which make the alloy have higher electrical

conductivity. Therefore, the influence factors of electrical conductivity of the rolled Cu–Ni–Mo alloy include dislocations, precipitates, grain boundaries, vacancy and gap atoms, under their comprehensive action, the electrical conductivity of the alloy is in a state of dynamic equilibrium with the change of rolling deformation, even after rolling with 60% and 80% deformation, the electrical conductivity of the alloy has no obvious change.

5. Conclusion

(1) The Cu–Ni–Mo ternary alloys-based on cluster model design was successfully prepared by aluminothermic reaction. The cluster of Ni and Mo atoms uniformly dissolves into the Cu matrix, but there is still a small amount of Mo precipitated because of the evaporation of a small amount of Ni during the reaction resulting in the ratio of Mo to Ni is greater than the solid solution cluster ratio of 1:12.

(2) The hardness and strength of as-cast Cu–Ni–Mo alloy increase with the increase of alloying element content, while the electrical conductivity decreases. Both the increase of strength and the decrease of conductivity are mainly caused by the content of solute atoms in Cu matrix.

(3) When the rolling deformation of Cu–Ni–Mo alloy is 40%, the grains and precipitates are elongated along the rolling direction. With the further increase of the rolling deformation, the grain elongated more obviously along the rolling direction, forming a larger ratio of lamellar structure, grain orientation tends to be the same. When the amount of deformation increases to 80%, the grain size decreases obviously, and a large number of fibrous deformation bands produced. The size of the initial precipitates also decreases obviously, and the distribution is more uniform.

(4) The dislocation density of Cu–Ni–Mo alloys increases significantly during the rolling process, causing stress concentration, hindering the movement of dislocations, resulting in dislocation plugging, and the size of the grains and precipitated phases after rolling are significantly refined, the distribution of the precipitated phases becomes more uniform. Under the combined effects of deformation strengthening, fine grain strengthening and precipitation strengthening, the strength and hardness are significantly increased, while the elongation is significantly reduced.

(5) The decrease of point defect concentration and precipitated phase size, the increase of distribution uniformity in rolled alloy all contribute to the improvement of conductivity in different degrees. But the dislocations proliferate with the rolling process, resulting in the decrease of electrical conductivity. Under this kind of comprehensive action, the resistivity always reaches a dynamic equilibrium with the change of rolling deformation, thus the electrical conductivity of the rolled alloys of different compositions has no obvious change.

Acknowledgments

We gratefully acknowledge the financial supports of the University Innovation Fund of Gansu Province in 2020 (Grant No. 2020A-030) and the Science and Technology Plan of Gansu Province (Grant No. 18YF1WA069).

References

1. J. Ruzic *et al.*, *Mater. Des.* **49** (2013) 746.
2. K. Maki *et al.*, *Scr. Mater.* **68** (2013) 777.
3. R. Mishnev *et al.*, *Mater. Sci. Eng. A* **629** (2015) 29.
4. Y. G. Ko *et al.*, *J. Alloys Compd.* **504** (2010) S448.
5. M. Murayama *et al.*, *J. Electron. Mater.* **35** (2006) 1787.
6. A. Akhtar and E. Teghtsoonian, *Acta Mater.* **17** (1969) 1339.
7. S. Lee *et al.*, *Mater. Sci. Eng. A* **799** (2020) 139815.
8. C. Zhu *et al.*, *J. Alloys Compd.* **582** (2014) 135.
9. D. N. Seidman *et al.*, *Acta Mater.* **50** (2002) 4021.
10. G. Purcek *et al.*, *Mater. Sci. Eng. A* **649** (2016) 114.
11. A. Kumar *et al.*, *J. Alloys Compd.* **653** (2015) 301.
12. I. Souli *et al.*, *Thin Solid Films* **647** (2018) 1040.
13. J. Zhang *et al.*, *Acta Mater.* **45** (2009) 1390.
14. J. Zhang *et al.*, *J. Alloys Compd.* **505** (2001) 179.
15. Y. Zheng *et al.*, *J. Mater. Res.* **30** (2015) 3299.
16. X. N. Li *et al.*, *Appl. Surf. Sci.* **89** (2014) 297.
17. H. Li *et al.*, *J. Phys. D: Appl. Phys.* **49** (2016) 035306.
18. X. N. Li *et al.*, *J. Electron. Mater.* **41** (2012) 3447.
19. P. Q. La *et al.*, *Phil. Mag. Lett.* **94** (2014) 478.
20. Z. N. Li *et al.*, *Mater. Lett.* **238** (2019) 191.
21. H. D. Wang *et al.*, *Metall. Mater. Trans. A* **45** (2014) 522.
22. M. Afifeh *et al.*, *Mater. Sci. Eng. A* **768** (2019) 138451.
23. M. Wang *et al.*, *Mater. Sci. Eng. A* **801** (2021) 140379.
24. L. Jia *et al.*, *Rare Metal Mater. Eng.* **47** (2018) 1980.
25. F. Torre *et al.*, *Metall. Mater. Trans. A* **38** (2007) 1080.
26. M. Ostafin *et al.*, *Arch. Metall. Mater.* **50** (2005) 409.
27. Q. Xing *et al.*, *Metall. Mater. Trans. A* **37** (2006) 1311.
28. P. P. Bhattacharjee *et al.*, *Mater. Sci. Eng. A* **459** (2007) 309.
29. P. P. Bhattacharjee *et al.*, *Metall. Mater. Trans. A* **44** (2013) 2707.
30. L. A. Barreiro *et al.*, *Physica A* **283** (2000) 160.
31. A. Takeuchi and A. Inoue, *Mater. Trans.* **46** (2005) 2817.
32. N. Hansen, *Mater. Sci. Technol.* **6** (1990) 1039.
33. T. S. Reddy *et al.*, *Intermetallics* **91** (2017) 150.
34. F. R. Fickett, *Cryogenics* **11** (1971) 349.
35. J. Marandel *et al.*, *Metall. Mater. Trans. A* **6** (1975) 449.
36. U. Sunkari *et al.*, *Mater. Sci. Eng. A* **769** (2020) 138489.
37. F. Lou *et al.*, *Chin. J. Nonferrous Met.* **4** (2001) 86.